

# Bulk etch rate measurements and calibrations of CR39 and Makrofol nuclear track detectors

V. Togo<sup>a</sup>, I. Traoré<sup>b</sup>, for the CERN-EMU-018 Collaboration\*

<sup>a</sup>INFN, Sezione di Bologna, Viale C. Berti Pichat 6/2, I-40127 Bologna, Italy

<sup>b</sup>Physics Department, FAST, University of Bamako, BP E2528, Bamako, Mali

## Abstract

We developed a new method for determining the bulk etch rate velocity based on both cone height and base diameter measurements of the etched tracks. This method is applied here for the calibration of CR39 and Makrofol nuclear track detectors exposed to 158 A GeV In<sup>49+</sup> and Pb<sup>82+</sup> ions, respectively. For CR39 the peaks corresponding to indium ions and their different fragments are well separated from  $Z/\beta = 7$  to 49: the detection threshold is at REL  $\sim 50$  MeV cm<sup>2</sup> g<sup>-1</sup>, corresponding to a nuclear fragment with  $Z/\beta = 7$ . The calibration of Makrofol with Pb<sup>82+</sup> ions has shown all peaks due to lead ions and their fragments from  $Z/\beta \sim 51$  to 83 (charge pickup). The detection threshold of Makrofol is at REL  $\sim 2700$  MeV cm<sup>2</sup> g<sup>-1</sup>, corresponding to a nuclear fragment with  $Z/\beta = 51$ .

**Key words:** Calibration; Bulk etch rate; Nuclear track detector.

## 1. Introduction

Nuclear Track Detectors (NTDs) are commonly used in many branches of science and technology [1, 2]. The isotropic poly-allyl-diglycol carbonate polymer, commercially known as CR39 is the most sensitive NTD; also Makrofol and Lexan polycarbonates are largely employed. More than 4000 m<sup>2</sup> of CR39 detectors were used in the MACRO and SLIM experiments devoted to the search for new massive particles in the cosmic radiation (magnetic monopoles, nuclearites, Q-balls) [3, 4, 5, 6, 7, 8, 9, 10, 11, 12]. Several experiments are going on in different fields which require an accurate detector calibration [13, 14]. A nuclear track detector can record the passage of ionizing particles or any highly charged particle via their Restricted Energy Loss (REL). The latent damage trail formed in NTDs may be enlarged by a suitable chemical etching and made visible under an optical microscope. The latent track develops into a conical-shaped etch-pit (Fig.1) when the etching velocity along the particle trajectory ( $v_T$ ) is larger than the one for the bulk etching of the material ( $v_B$ ) [15]. The sensitivity of NTDs crossed by particles with constant energy loss can be characterized by the ratio  $p = v_T/v_B$  (reduced etch rate) which may be determined by measuring the bulk etch rate  $v_B$  and either the etch-pit diameter or the etch-pit height. Two methods have been used to determine  $v_B$ . The first is the common one based on the mean thickness difference determination before and after etching. The second method that is the main aim of this paper, is based on both cone height and base diameter measurements of the etched tracks.

## 2. Experimental

### 2.1. Detectors and exposure

A stack composed of Makrofol and CR39 foils of size 11.5 x 11.5 cm<sup>2</sup> with a 1 cm thick lead target was exposed to 158 A GeV Pb<sup>82+</sup> ions in 1996 (Pb96); a second stack with a 1 cm thick aluminium target was exposed to 158 A GeV In<sup>49+</sup> ions in 2003 (In03); both exposures were performed at the CERN-SPS, at normal incidence and a total ion density of  $\sim 2000/\text{cm}^2$ .

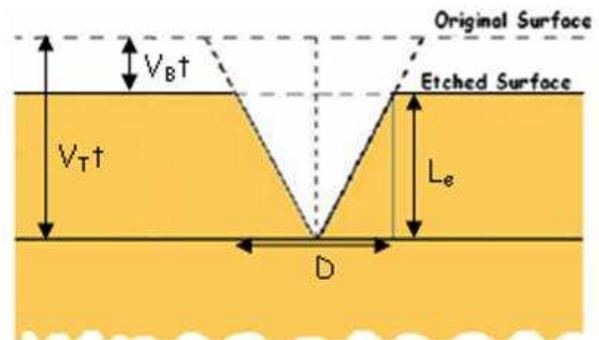


Figure 1: Sketch of an etched track for a normally incident ion in a nuclear track detector.

The detector foils downstream of the target recorded the beam ions as well as their nuclear fragments [16, 17, 18], see Fig2. The CR39 polymer sheets used in the present study were manufactured by Intercast Europe Co., Parma, Italy where a specific production line was set up in order to achieve a lower

\*The CERN-EMU-018 Collaboration: A.Bâ, S.Balestra, M.Cozzi, G.Giacomelli, R.Giacomelli, M.Giorgini, A.Kumar, G.Mandrioli, S.Manzoor, A.R.Margiotta, E. Medinaceli, L.Patrizii, V.Popa, I.E.Qureshi, M.A.Rana, Z.Sahnoun, G.Sirri, M.Spurio, V.Togo, I.Traoré, C.Valieri

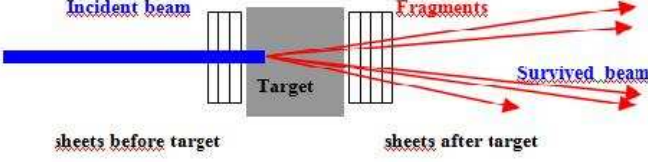


Figure 2: Exposure set-up for the calibration of CR39 and Makrofol NTDS.

detection threshold, a higher sensitivity in a larger range of energy losses, a high quality of the post-etched surfaces after prolonged etching [19, 20, 21, 22]. The Makrofol detectors were manufactured by Bayer A.G., Germany. They have a thickness of 500  $\mu\text{m}$ . The CR39 thickness is either 700  $\mu\text{m}$  or 1400  $\mu\text{m}$ . All detector sheets were covered by a 30  $\mu\text{m}$  plastic film to protect them from exposure to ambient radon; the protective layers were removed before etching.

## 2.2. Etching conditions

After exposures, two CR39 foils and two Makrofol foils located after the target were etched. The etchant used were 6N NaOH or 6N KOH at temperatures in the range from 45°C to 70°C and different etching times. The addition of ethyl alcohol in the etchant [23] improves the etched surface quality, reduces the number of surface defects and background tracks, increases the bulk etching velocity, speed up the reaction, but raises the detection threshold [10, 24]. It results that 6N NaOH + 1% ethyl alcohol at 70°C for 40 h and 6N KOH + 20% ethyl alcohol at 50°C for 8 h represent the optimum etching condition for CR39 and Makrofol, respectively. The etching was performed in a stainless steel tank equipped with internal thermostances and a motorized stirring head. In order to keep homogeneous the solution and to avoid that etched products deposit on the detector surfaces, a continuous stirring was applied during etching. The temperature was stable to within  $\pm 0.1$  °C. For CR39 detectors, etch-pit base diameters and heights of In ions and their fragments were measured with a Leica optical microscope. In Makrofol, Pb ions and their high Z fragments ( $Z > 77$ ) made through-holes in the detector sheets; thus the cone length  $L_e$  was measured only for fragment tracks that have sharp etch-cone tips (no holes). Nuclear fragments with Z charges  $78 \leq Z \leq 82$  were identified by etching another Makrofol sheet from the same stack in the same conditions but for only 5 h.

## 2.3. Bulk etch rate from the thickness-changing measurements.

For the determination of  $v_B$ , the thickness of the detectors was measured in 25 selected points with an electronic micrometer of 1  $\mu\text{m}$  accuracy. The average bulk etch velocity is  $v_B = \Delta x / 2\Delta t$ , where  $\Delta x$  is the mean thickness difference after a  $\Delta t$  etching time. For CR39, at etching time shorter than 10 h the thickness is affected by detector swelling [25, 26, 27]. For Makrofol no significant swelling effect was observed.

## 2.4. Bulk etch rate from the cone height and base diameter measurements

For relativistic charged particles the track etch rate  $v_T$  can be considered constant. For normally incident particles, the measurable quantities are the cone base diameter D, and the height  $L_e$  [24] see Fig1. The following relations hold:

$$L_e = (V_T - V_B)t \quad (1)$$

$$D = 2V_B t \sqrt{\frac{(V_T - V_B)}{(V_T + V_B)}} \quad (2)$$

From the above relations, the following quadratic equation in  $v_B$  is obtained:

$$\left(\frac{L_e}{t}\right)V_B^2 - \left(\frac{D^2}{2t^2}\right)V_B - \left(\frac{D^2 L_e}{4t^3}\right) = 0 \quad (3)$$

The real solution for  $v_B$  is:

$$V_B = \frac{D^2}{4tL_e} \left[ 1 + \sqrt{1 + \frac{4L_e^2}{D^2}} \right] \quad (4)$$

From Eq.(1) the track etch rate  $v_T$  can be written as:

$$V_T = V_B + \frac{L_e}{t} \quad (5)$$

From Eqs. (1) and (2), the reduced etch rate follows:

$$P = \frac{V_T}{V_B} = 1 + \frac{L_e}{V_B t} = \frac{1 + \left(\frac{D}{2V_B t}\right)^2}{1 - \left(\frac{D}{2V_B t}\right)^2} \quad (6)$$

We may thus determine the bulk etch rate  $v_B$  and the reduced etch rate p by measuring the track parameters  $L_e$  (measured with a precision of  $\sim 1$   $\mu\text{m}$ ) and D (precision of 0.5  $\mu\text{m}$ ).

Relations (4) and (6) were tested with relativistic Pb and In ions and their nuclear fragments. We selected only tracks for which precise measurements of the cone height and diameter could be performed (for example we cannot measure the track cone heights for low Z fragments, for which the microscope image may be affected by shadow effects). Then, using Eq. (4) we computed the bulk etch rate for CR39 and Makrofol. Batches of measurements were made by different operators, and the average  $v_B$ 's and their statistical standard deviations were computed, see Table 1. By this method we obtain  $v_B$  values with accuracies of  $\pm 0.01$  to 0.05  $\mu\text{m}/\text{h}$ . The  $v_B$  values obtained for the same foils using detector thickness measurements are also given.

Detector (beam)	Z range	Etching conditions	$V_B$ new method ( $\mu\text{m}/\text{h}$ )	$V_B$ thickness method ( $\mu\text{m}/\text{h}$ )
CR39(In03)	44-49	6N NaOH+1% alcohol, 70°C, 40h.	$1.25 \pm 0.01$	$1.15 \pm 0.03$
CR39(Pb96)	75-80	6N NaOH 70°C, 30h.	$1.10 \pm 0.02$	$1.15 \pm 0.03$
CR39(Pb96)	78-82	6N NaOH 45°C, 268h.	$0.16 \pm 0.01$	$0.17 \pm 0.03$
Makrofol(Pb96)	75-78	6N KOH+20% alcohol, 50°C, 8h.	$3.44 \pm 0.05$	$3.52 \pm 0.13$

Table 1: Bulk etch rates  $v_B$  for CR39 and Makrofol NTDs obtained with the new and the thickness-changing methods. The errors are statistical standard deviations of the mean. The different values of  $v_B$  for Pb96 in rows 3 and 4 are due to the different etching temperatures.

### 3. Calibrations

In the following sections calibration data based on the new determination of the bulk etch rate for Makrofol exposed to  $\text{Pb}^{82+}$  ions and CR39 exposed to  $\text{In}^{49+}$  ions are reported. The calibration is given as a relation between the reduced etch rate  $p$  and the particle restricted energy loss (REL) [28, 29].

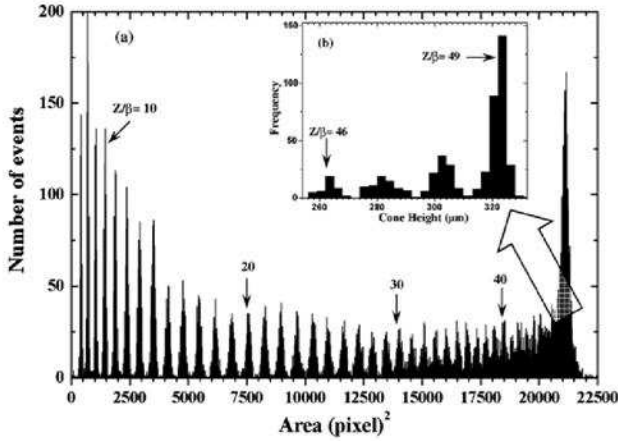


Figure 3: Base area distribution of etched cones in CR39 from 158 A GeV  $\text{In}^{49+}$  ions and their fragments (averages of two front face measurements). In the insert are shown the cone height distributions for  $46 \leq Z/\beta \leq 49$ . Etching conditions: 6N NaOH+1% ethyl alcohol, 70°C, 40 h.

#### 3.1. Calibration of the CR39 detector

Fig.3 shows the etch-pit base area distribution for indium ions and their fragments in CR39 measured with the Elbek automatic image analyzer system [30]; averages were computed from measurements made on the front sides of two detector sheets. The peaks are well separated from  $Z/\beta \sim 7$  to 45; the charge resolution for the average of two measurements is  $\sigma_z \sim 0.13e$  at  $Z/\beta \sim 15$ . The charge resolution close to the indium peak ( $Z \sim 49$ ) can be improved by measuring the heights of the etch-pit cones [31]. The height of 1000 etch-cones with diameter larger than  $48 \mu\text{m}$  (corresponding to nuclear fragments with  $Z > 45$ ) were measured with an accuracy of  $\pm 1 \mu\text{m}$  with a Leica microscope coupled to a CCD camera and a video monitor. The corresponding distribution is shown in the insert in Fig.3; each of the four peaks is well separated from the others, and a charge can be assigned to each one [32]. For each detected

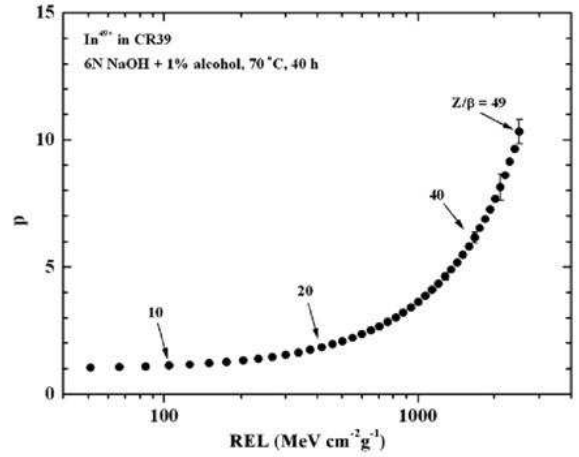


Figure 4:  $p$  versus REL for CR39 exposed to relativistic indium ions using  $v_B$  evaluated with the new method. Typical statistical standard deviations are shown at  $Z/\beta = 40, 45, 49$ ; for  $Z/\beta = 37$  the errors are smaller than the black points.

nuclear fragment from  $Z/\beta = 7$  to 48 and indium ions ( $Z = 49$ ) we computed the REL and the reduced etch rate  $p = v_T/v_B$  using Eq. (6);  $p$  versus REL is plotted in Fig.3; the CR39 detection threshold is at  $\text{REL} \sim 50 \text{ MeV cm}^2 \text{ g}^{-1}$  (corresponding to a relativistic nuclear fragment with  $Z \sim 7$ ).

#### 3.2. Calibration of the Makrofol detector

Fig.5 shows the base area distribution for the average of two measurements of Pb ions and their fragments in Makrofol; averages were computed from measurements on the front sides of two detector foils. The peaks are well separated from  $Z/\beta \sim 51$  to  $\sim 77$  (the charge resolution is  $\sigma_z \sim 0.18e$  at  $Z/\beta \sim 55$ ). The charge resolution close to the Pb peak ( $Z = 82$ ) was improved by measuring the heights of the etch-pit cones. The heights of 4000 etch cones with base diameter larger than  $47 \mu\text{m}$  were measured [33]; the corresponding distribution is shown in the insert in Fig.5; each peak is well separated from the others, and a charge was assigned to every peak.

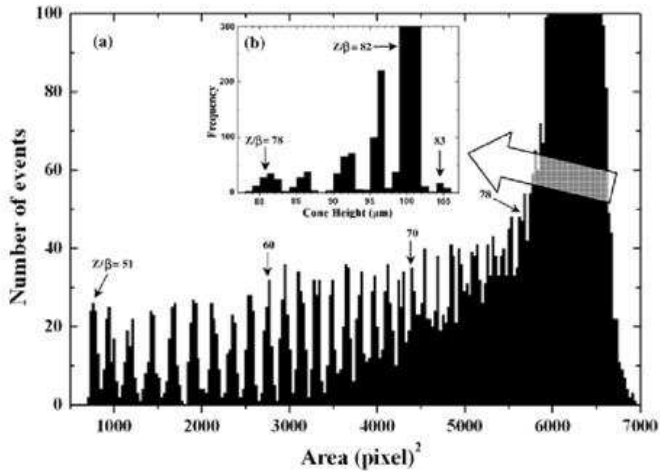


Figure 5: Base area distribution of etched cones in Makrofol from 158 A GeV  $Pb^{82+}$  ions and their fragments (averages of two front face measurements). Etching conditions: 6N KOH+20% ethyl alcohol, 50°C, 8 h. In the insert are shown the cone height distribution for  $78 = Z/\beta = 83$ . Etching conditions: 6N KOH+20% ethyl alcohol, 50°C, 5 h.

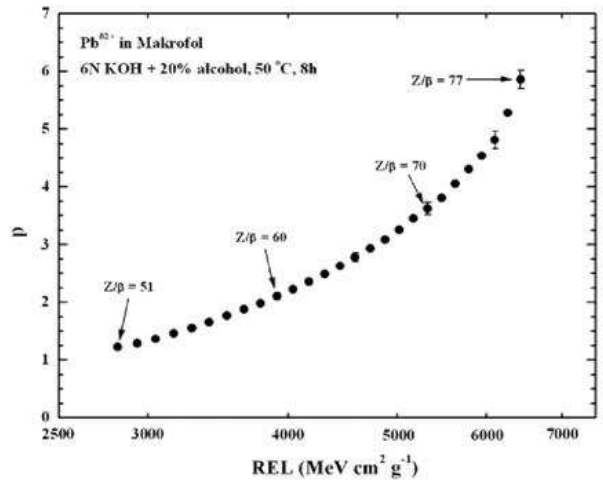


Figure 6:  $p$  versus REL for the Makrofol detector exposed to relativistic Pb ions using  $v_B$  evaluated with the new method. Typical statistical standard deviations are shown at  $Z/\beta = 70, 75, 77$ ; for  $Z/\beta = 67$  the errors are smaller than the black points.

#### 4. Discussion and Conclusions

We have studied the response of CR39 and Makrofol NTDs to relativistic indium and lead ions and their fragments using measurements of the etch-pit base area and of the heights of the etch-pit cones. The bulk etch rate measurements using the new method yields slightly smaller uncertainties than the standard method (change in thickness). The distributions of the peaks for the primary ions and for their fragments are given in Figs.3 (for CR39) and 5 (for Makrofol). At low  $Z/\beta$  the measurements of the etch-pit base area are adequate; it is seen that for high  $Z/\beta$ , the base area distribution does not give well separated peaks, while by cone height measurements the peaks are well separated (see the inserts in Figs. 3 and 5). The reduced etch rate  $p$  (computed with the new method) plotted versus REL covers a large  $Z/\beta$  range for both detectors, Figs.4 (for CR39) and 6 (for Makrofol).

#### Acknowledgments

We thank the CERN SPS staff for facilitating the Pb and In beam exposures. We acknowledge many colleagues for their cooperation and technical advice. We gratefully acknowledge the contribution of our technical staff in Bologna. We thank INFN and ICTP for providing fellowships and grants to non-Italian citizens.

#### References

[1] Fleischer, R.L., et al., Nuclear Tracks in Solids, University of California Press, Berkeley, 1975.

[2] Durrani S.A., et al., Solid State Nuclear Track Detection, Pergamon Press, Oxford, 1987.  
 [3] Ambrosio, M., et al., Eur. Phys. J. C 25, 2002, 511. hep-ex/0207020  
 [4] Ambrosio, M., et al. Nucl. Instr. Meth. A 486, 2002, 663.  
 [5] Balestra, S., et al., Eur. Phys. J. C 55, 2008, 57.  
 [6] Cecchini, S., et al., astro-ph/0510717, 2005.  
 [7] Cecchini, S., et al., Radiat. Meas. 40, 2005, 405.  
 [8] Derkaoui, J., et al., Astropart. Phys. 10, 1999, 339.  
 [9] Giacomelli, G., et al., hep-ex/0702050, 2007.  
 [10] Manzoor, S., et al., Nuclear Physics B (Proc. Suppl.) 172, 2007, 296.  
 [11] Medinaceli, E., et al., this Conference.  
 [12] Sahnoun, Z., et al., this Conference.  
 [13] Uchihori, Y., et al., J. Radiat. Res. 43 (Suppl. S81-5) 2002.  
 [14] Kodaira, S., et al., Jpn. J. Appl. Phys. 43, 2004, 6358.  
 [15] Nikezic, D., et al., Material Science Eng. R46, 2004, 51.  
 [16] Cecchini, S., et al. Nucl. Phys. A 807, 2008, 206.  
 [17] Giorgini, M., et al., 2008. this Conference.  
 [18] Togo, V., et al., Nucl. Instr. Meth. A 580, 2007, 58.  
 [19] Ahlen, S.P., et al., Int. Journal Radiat. Appl. Instr. Part D. 19, 1991, 64.  
 [20] Fantuzzi, E., et al., Radiat. Meas. 36, 2003, 475.  
 [21] Patrizii, L., et al., Nucl. Tracks Radiat. Meas. 19, 1991, 641.  
 [22] Vilela, E., et al., Radiat. Meas. 31, 1999, 437.  
 [23] Matiullah, S., et al., Radiat. Meas. 39, 2005, 337.  
 [24] Balestra, S., et al., Nucl. Instr. Meth. B 254, 2007, 254.  
 [25] Ahlen, S.P., et al., Nucl. Instr. Meth. A 324, 1993, 337.  
 [26] Kumar, A., et al., Nucl. Instr. Meth. B 119, 1996, 515.  
 [27] Malik, F., et al., Radiat. Meas. 35, 2002, 301.  
 [28] Baiocchi, P., et al., Radiat. Meas. 25, 1995, 145.  
 [29] Cecchini, S., et al., Il Nuovo Cimento 109 A, 1996, 1119.  
 [30] Noll, A., et al., Nucl. Tracks Radiat. Meas. 15, 1988, 265.  
 [31] Giacomelli, G., et al., Nucl. Instr. Meth. A 411, 1998, 41.  
 [32] Cecchini, S., et al., Astropart. Phys. 1, 1993, 369.  
 [33] Manzoor, S., et al., Radiat. Meas. 40, 2005, 433.